Eduardo E. Alonso · Núria M. Pinyol

Slope stability in slightly fissured claystones and marls

Abstract The paper deals with the behavior of some characteristic soft rocks found in the Iberian Peninsula. In geological terms, they belong to Tertiary basins, the Keuper period and the Jurassic-Cretacic transition. The discussion is organized around the following aspects: (a) the intact material and its brittle behavior; (b) the weathering action of atmospheric events; (c) the persistent discontinuities and scale effects; and (d) the modification of strength after failure. In all cases, instability phenomena are addressed in connection with several case histories. Regarding material brittleness and the initial stress state, two cases of first time failures are discussed. Practical implications concerning the selection of operative strength will be given. Field observations of the relevance of weathering and, also, on the rate of weathering, are given for a Weald claystone. Field observations emphasize the importance of sharp transitions between weathered and intact (or slightly weathered) levels. A recent long-term laboratory investigation on the nature of degradation will be summarized. Macroscopic variables such as stiffness and tensile strength have been found to be uniquely predicted by a degradation law in terms of the accumulated plastic deformations. Persistent discontinuities and, in particular, sedimentation planes play a dominant role to explain slope failures not related to the shallow failures, usually associated with weathered profiles. The strength of discontinuities in a Weald formation was investigated by means of tests performed at two scales. Finally, the evolution in time of residual strength induced by chemical actions, associated with groundwater flow, is highlighted in connection with actual field data of unstable slopes.

Keywords Slope instability · Claystone · Weathering · Discontinuities · Scale effects · In situ tests · Case history

Introduction

This paper concentrates on slope problems in natural formations of the Iberian Peninsula. A significant part of the territory is occupied by Tertiary sedimentary basins (Fig. 1). These basins, drained by the longest rivers in Spain, are filled by horizontally layered sequences of claystones, including marls, siltstones, sandstones, and limestone banks. The exposed slopes of the river valleys offer the possibility of observing the sequence of these materials. Figure 2 provides one example of horizontally layered Oligocene strata. The exposed claystones often exhibit a varying degree of cementation that explains the resistance to weathering. When submerged in water, these materials may degrade very fast or resist essentially unharmed. Variable cementation coexists often in a given location. Horizontal layering leads to stable slopes in general terms, and this is the situation prevailing in the central areas of the valleys. However, folding and faulting are more common in basin boundaries, and slope stability problems become more frequent.

Figure 1 also shows the extent of the Mesozoic basement of the Peninsula. It characterizes also much extended areas, especially in the eastern part of Spain. Some specific Mesozoic geologic units are well known for their susceptibility to generate landslides at different scales: the Keuper (Triassic) materials, the Weald facies at the Jurassic-Cretaceous transition, and the Garum facies at the end of the Jurassic period. These are claystones and siltstones that have experienced, if compared with deposits of Tertiary basins, a more intense tectonic action. One example of these materials is given in Fig. 3: A Weald claystone found in the foundation excavation for Castrovido dam in Burgos. Paleozoic rocks, also represented in Fig. 1, are left outside this paper.

It is unrealistic to try to define a common set of geotechnical properties for these materials. However, a number of features that help to introduce the discussion could be mentioned:

- Carbonates and sulfates are often present in variable proportions.
- Discontinuities at a large scale (sedimentation planes, faulting, and joints) play very often a significant role in slope stability (Skempton and Petley 1967; Morgenstern 1977; Dixon and Bromhead 1991; Mesri and Shahien 2003). Their behavior is a key piece of information in many cases.
- Dense microfissuring is sometimes observed, but this is not a very common feature in the geologic formations mentioned.
- The clay or silt matrix exhibits a brittle behavior when sheared. This is a consequence of overconsolidation and cementation. The initial state of stress (before excavation, in the case of open cuts) is seldom investigated, but it plays a very relevant role to explain stability conditions. One may suspect that K_o values in excess of 1.5–2 are the rule. Both factors (brittleness and high K_o) imply that progressive failure should be a widespread phenomenon in first time failures. A recent analysis of the effect of K_o and brittleness on the failure of Guadalquivir overconsolidated, plastic, marine blue clays, of Miocene age, is given by Zabala and Alonso (2011).
- Their permeability may be very low, especially when the clay exhibits a high plasticity. Medium to low plasticity materials dominate.
- Lack of saturation is very common, because of the semi-arid or arid climates in most of the Iberian Peninsula, especially in central and eastern regions. More precisely, suction changes induced by direct atmospheric action result in major irreversible changes in porosity and strength, which explain slope failures in exposed surfaces. These are processes developing in time, and they are superimposed to the effect of stress changes (in case of excavations) and dissipation of pore pressures.
- The reactivation of old landslides is generally accepted to involve the residual strength along the (ancient) failure surface. However, there is evidence showing that chemical processes lead to a modification of the laboratory measured residual strength. Any process leading to a change of the clay content and clay mineralogy in the sliding surface
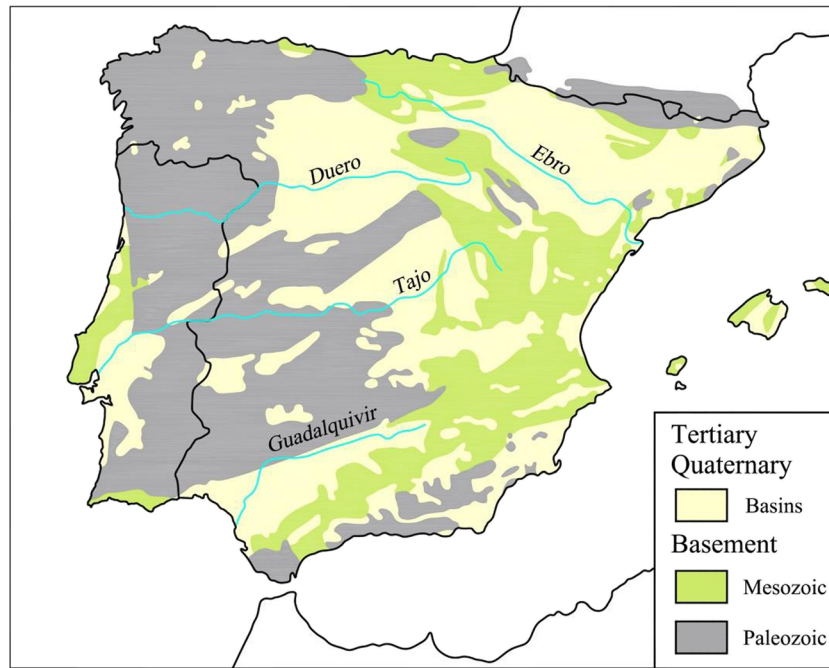
Fig. 1 Simplified geological map of Iberian Peninsula

will lead to a modification of shear strength (Mesri and Huvaj-Sarihan 2012).

Some of these features will be described in the paper and discussed further in connection with some slope stability case histories.

The discussion is organized around four topics:

– Material brittleness and progressive failure (first time failures)
– Weathering
– Discontinuities
– The modification of strength after failure (landslide reactivation)

Material brittleness and progressive failure events

Sabadell cut

Figure 4 shows a slope failure triggered by an excavation at the toe of a relatively gentle slope (~12°). The cross section in Fig. 5 shows the sequence of Tertiary claystones, siltstones, and lightly cemented sands of Tertiary origin which characterize the slope. These are hard soils that could only be sampled by rotary coring.

Inclinometer readings (the position is given in Fig. 5), taken immediately after the failure, indicated a slope creeping motion that allowed the identification of a well-marked failure surface at a

Fig. 2 Claystone and sandstone layers, horizontally layered, in Albagés, Lleida, Ebro basin

Fig. 3 A sedimentation plane in Castrovido Weald claystone. Despite the sheared aspect of this surface, there were indications of a sin-sedimentary feature. If this interpretation is correct, the observed geometry is a consequence of early deformations, including some shearing, at the time of deposition

claystone-siltstone contact, which followed the inclination of sedimentary layers. It was clear that the excavation favored the development of a planar motion, which daylighted at the toe of the excavated slope.

Plasticity of the claystone was medium to high (w_L=48 to 56 %; w_P=20 to 23 %) and "in situ" water content (w=26 to 28 %) was close to the plastic limit. A series of direct and ring shear tests in remolded samples allowed the determination of the strength envelopes shown in Fig. 6. The plot shows the brittle behavior of the claystone. The minimum residual friction angle determined was close to the natural slope inclination and also to the dip angle of the sequence of strata. No indication of pore water pressures was found. In fact, four of the borings drilled after failure were equipped with Vibrating Wire Piezometers located at increasing

depths (7.5 to 24 m; three sensors per boring). In no case, positive pore water pressures were recorded in a few weeks following the failure. No significant rainfall was either measured in the weeks previous to failure. The strongest daily rainfall was 17 l/m² during this period, and the sequence of relatively impervious layers parallel to the exposed ground surface made an unexpected increase of rainfall-induced pore water pressure very unlikely.

The case is interesting because equilibrium was achieved for a friction angle similar to the minimum measured residual friction angle. Stabilization was achieved by a pile barrier that was designed accepting that the minimum residual friction angle was operating on the shearing surface. The failure surface was probably located within the high plasticity claystone layer (Fig. 5).

The measured strength envelopes indicate that failure was most probably preceded by a progressive failure mechanism induced by the excavation. Tertiary deposits in the region are known to exhibit high horizontal stresses. In an investigation of the "in situ" stresses in a shallow tunnel excavated in Tertiary claystones in the neighboring city of Tarrassa, Gens et al. (1996) reported the K_o values of 1.7–2.2. A previous "damage" (slip contact) of the shearing strength of sedimentary planes may also explain the failure, but no evidence of striations was found in the cores recovered or in the visual inspection of the exposed slope.

Viladesens embankment failure

In May 2004, 200 m of a motorway embankment in the Province of Girona (Viladesens in the remaining description) experienced a progressive instability that forced the interruption of traffic. The embankment was built 30 years before and no significant incidents were recorded except for some occasional settlements. Figure 7 shows the head of the slide which destroyed one of the motorway lanes. The embankment was built on a natural clayey slope of gentle inclination (8°). The failure was unexpected because of the long period of stability after construction.

However, the nature of the natural soil, overconsolidated high plasticity clay, suggests that a slow creeping motion combined with a progressive failure mechanism could have played a critical role.
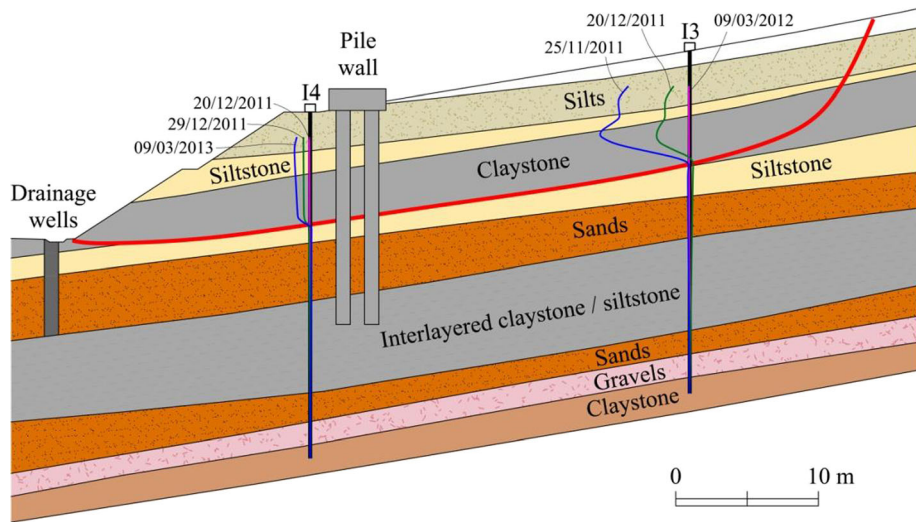

Fig. 4 Sabadell slope failure

Fig. 5 Sabadell slope failure. Cross section along slide axis. The position of the sliding surface, inclinometers and remedial stabilizing measures (pile wall) are indicated

Figure 8a shows a representative cross section of the embankment. The sliding surface was located, by interpreting inclinometer readings, close to the contact between the compacted embankment and the brown stiff natural clay. The slide may be described as a translational motion essentially parallel to the natural slope. A water table was also identified in the lower third of the embankment height. During the months prior to failure, intense rainfalls were reported.

Borings performed immediately after the first cracks were detected on the pavement identified a substratum described as stiff, sometimes hard, overconsolidated, and fissured clay. Sand lenses were also detected in the upper levels of the natural formation, close to the embankment contact. These pervious materials may have contributed to increase the water pressure on the embankment-natural clay interphase.

Liquid limits in the range 50−100 % were measured. Natural water content (21–22 %) was lower than plastic limit (29–30 %). Void ratios ranged from 0.5 to 0.65. In cores recovered, slickensided surfaces (Fig. 8b) were also observed. Direct shear tests were
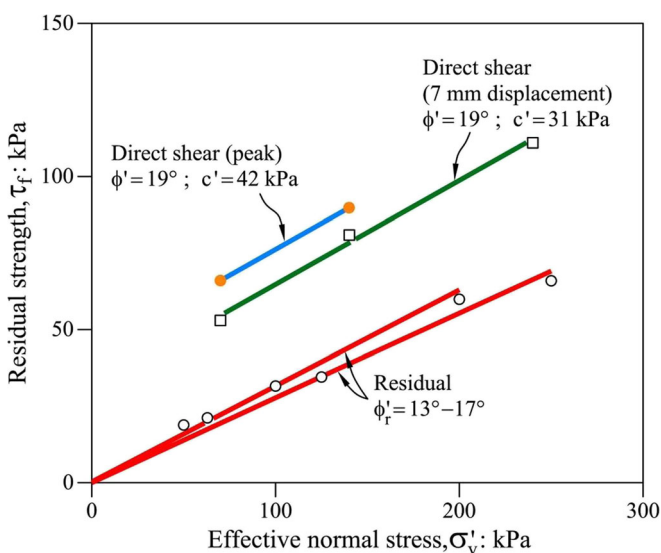
performed on cores. Residual strength was also measured in a ring shear device. Some results are given in Fig. 9.

Intact core samples tested on direct shear tests exhibited a marked brittle nature. Peak strengths were reached for relative shear displacements close to 1 mm. Positive (expansion) dilatancy rates were also recorded.

There was a particular interest in investigating the residual strength conditions that should prevail at the embankment-natural clay contact after failure. Figure 9 collects data from three different sources: the ring shear test, some direct shear tests performed on natural slickensided joints, and the strength measured on direct shear tests on cores for large relative displacements (∼6 mm). Also given in the figure are the peak strength points (stress ratios) measured in direct shear tests on cores.

The minimum residual friction was found in ring shear tests on remolded material ($\phi'_{res} \cong 9°$). This friction angle is equal to the natural slope inclination.

The back analysis of the failure provided friction angles for the embankment-clay contact slightly above the minimum residual friction mentioned before. A reasonable estimate was $\phi' \cong 11.5°$. Therefore, it was expected that additional slide displacements, once the slope was stabilized, could reduce somewhat the available basal resistance.

Aznalcóllar failure

Aznalcóllar dam failure was a case of sliding of the dam and an upper slab of foundation soil on a high plasticity overconsolidated marine Miocene clay. It has been described in a number of papers (Alonso and Gens 2006a, b; Gens and Alonso 2006; Zabala and Alonso 2011). The failure represented in Fig. 10 was attributed to the persistence of high load-induced pore water pressures in the foundation clay, the brittle behavior of the clay, and the "down-stream" construction method of the dam, which generate high shear stresses under the evolving dam toe. Aznalcóllar is a good example of a progressive failure phenomenon, analyzed in Zabala and Alonso (2011). Figure 11 is taken from this reference and shows the predicted position of the shearing band, eventually transformed into a full failure surface, when the dam reached a height of 25 m, 2 m below the dam height at the time of collapse.

Fig. 6 Shear tests on Sabadell slope claystone

Fig. 7 Scarp of Viladesens slide. May, 2004

Discussion

One important issue in practice is to predict the average friction angle leading to instability in the sense of a limit equilibrium analysis. This question has been discussed by some authors and
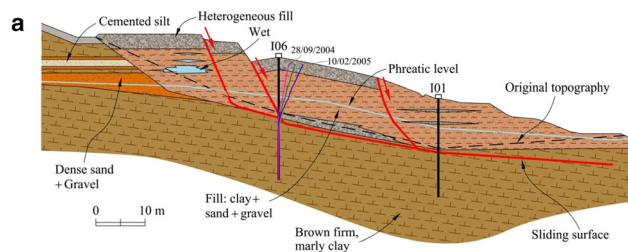

Fig. 8 Viladesens slide. **a** Cross section; **b** striated and polished surface in brown clay observed in recovered cores

also in the case of Aznalcóllar. An answer is given in Fig. 14, which shows results complied by Stark and Eid (1997) and the slope stability results of the case of Aznalcóllar.

The plot shows, for back analyzed cases reported by Stark and Eid (1997), the stress ratio mobilized at failure and two additional values for each of the cases represented: the so-called "fully softened stress ratio" and the residual stress ratio.

Samples of Guadalquivir clay were remolded and tested in a direct shear box at a very low strain rate and under different vertical effective confining stress. The stress ratio measured for the average effective stress in the central part of the slide (around 300 kPa) is 0.47, equivalent to a friction angle of 25°. This value is very close to the peak and post-peak friction angle measured on intact samples. This result suggests that the post-peak (at small additional straining) friction of intact samples may approximate the peak friction angles of remolded samples. A possible explanation is that in both cases the clay retains a random non-oriented microstructure of clay platelets and aggregates.

The remolded, mobilized, and residual friction angles in the case of Aznalcóllar are plotted also in Fig. 12, in terms of the liquid limit. Data for the previously described Sabadell and Viladesens failures are also included in the plot. In the case of Viladesens, an average liquid limit (w_L=75 %) was selected to plot the friction data.

The data by Stark and Eid (1997) and Aznalcóllar tend to indicate that the prevailing average friction at failure is halfway between fully softened (or peak) and residual friction angles. Other contributions supporting the fact that a mobilized shear strength of claystones may be at an intermediate value between the fully softened strength and residual strength have been reported by Chandler (1984), Mesri and Abdel-Ghaffar (1993), and Potts et al. (1997). However, there is nothing fundamental in this observation. The mobilized (average) friction angle at failure depends on many aspects (pore pressure generation and dissipation,
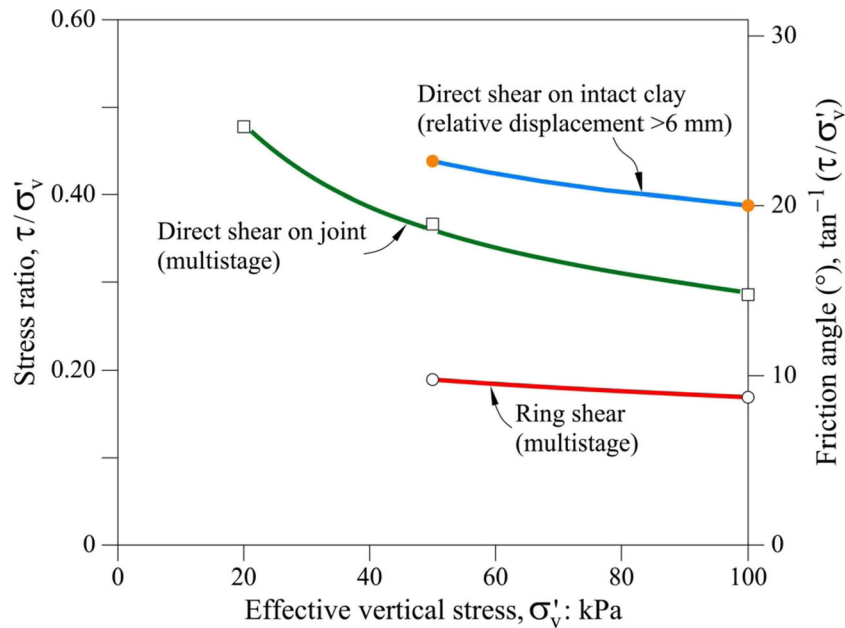
Fig. 9 Stress ratios and secant friction angles for different shearing conditions. Viladesens clay

clay brittleness, initial stress state...) and also on the external actions leading to the slope failure. The cases of Sabadell and Viladesens also plotted in Fig. 12 are two extreme cases.

Sabadell is a first time failure induced by a rapid excavation in a highly stressed Tertiary formation. The failure took place along a sedimentary plane between a high plasticity claystone and a siltstone. Differential displacements of tectonic origin tend to concentrate on surfaces which are a boundary between layers of different stiffness. This may be the case in the Sabadell.

Then the sliding surface followed a partially damaged contact. Mesri and Shahien (2003) concluded that in many first time failures a large proportion of the sliding surface may be at the residual condition. The high initial horizontal stress identified in these Tertiary formations certainly contributes to reduce further the available shear strength due to a progressive failure mechanism. The slope has not yet been analyzed in detail to take into account the expected high K_o value and the strain softening behavior of the plastic claystone.
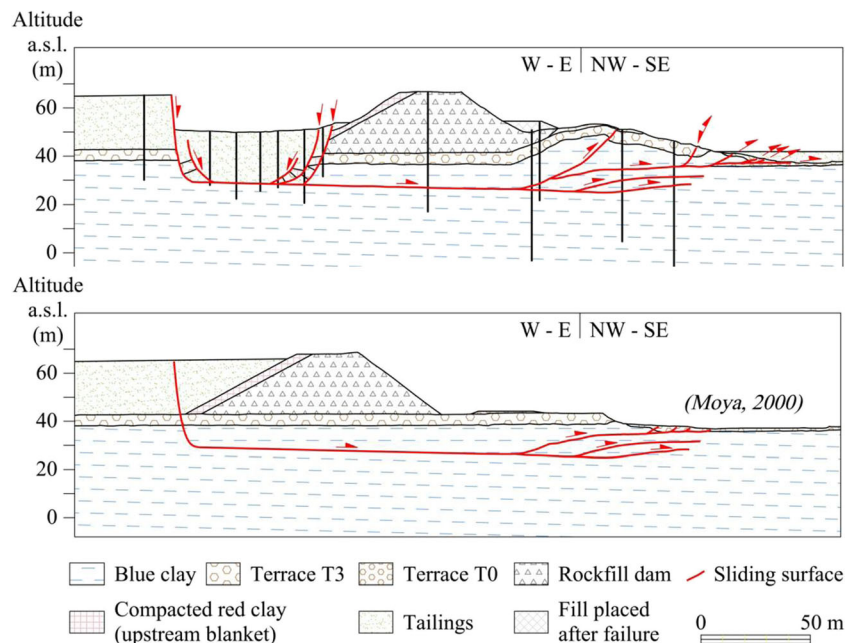

Fig. 10 Cross section of Aznalcóllar slide: **a** geometry after slide, as interpreted from borehole data and surface topography; **b** reconstruction of position of sliding surface before failure (Alonso and Gens 2006a)
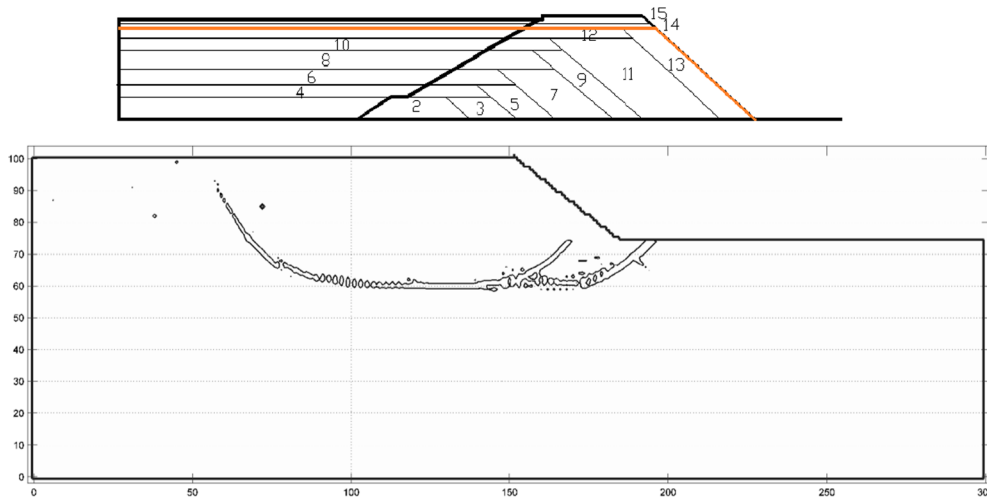
Fig. 11 Development of the failure surface. The plot shows the contours of equivalent plastic strain calculated in the foundation of clay when the dam reached a height of 25 m $K_0 = 1$ (Zabala and Alonso 2011)

Viladesens is a long-term failure induced by an embankment loading. In both cases, the average mobilized friction angle was found to be very close or equal to the residual strength. These two cases suggest that unless a careful analysis able to handle progressive failure is made, a conservative attitude should be adopted when selecting the mobilized average friction in brittle overconsolidated high plasticity clays.

Weathering

Weathering induced by atmospheric cycles on clayey rocks invariably lead to an increase in porosity and loss of stiffness and strength. Mechanical and chemical reasons explaining the deterioration of shear strength of claystones have been reported by several authors (Terzaghi 1936; Bjerrum 1967; Wilson 1970; Skempton 1970; Morgenstern 1977; Hutchinson 1988). Creeping, suction cycles (highlighted below), and freezing-thawing cycles (of limited intensity in the Iberian Peninsula) also contribute to claystone degradation (Chandler 1972; Tavenas and Leroueil 1981; Graham and Au 1985).

Vertical profiles of P or S waves are useful to identify the thickness and intensity of weathering. An example is given in Figs. 13 and 14 in connection with the foundation of a large gravity dam (Castrovido dam). Figure 13a shows a schematic plan view of an excavation in Weald claystones and the position of P-wave seismic profiles on the right margin of the river valley. Profiles PS-1 and PS-2 are located on the bottom of the excavation (8 m deep on average), whereas profiles PS-11 and PS-12 are located on natural undisturbed ground a few meters upstream of the PS-1 and PS-2 profiles. The purpose of this arrangement was to compare a long-term weathering action (PS-11 and PS-12) and a short-term exposure to atmosphere (PS-1 and PS-2). Short-term here means 3 years because the excavation remained open a relatively long-time because of administrative reasons.

The P-wave seismic profiles are given in Fig. 16b and c. Long-term natural weathering (Fig. 13b) reaches deeper levels than the short-term (3 years) exposure to atmosphere (Fig. 13c). This is better appreciated if vertical profiles of P-wave velocity are compared at
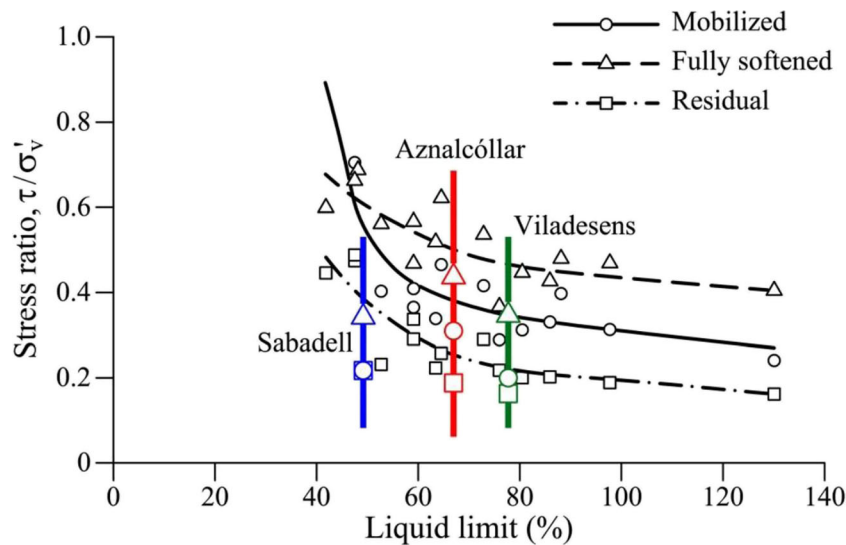

Fig. 12 Mobilized, fully softened, and residual stress ratio for field case histories (data from Stark and Eid 1997; Alonso and Gens 2006a; and present paper)

two given positions (profiles "C" and "D" in Fig. 13b and c). The comparison is shown in Fig. 14. In both cases, all profiles show a distinct pattern: the rate of increase of V_p with depth is relatively high in the upper levels and decreases to a lower, approximately constant value at depth. The deep trend of V_p increase with depth may be interpreted as an indication of undisturbed claystone. Then, the plots in Fig. 14 may indicate some maximum depth of the weathering action (7–10 m in the excavated abutment and 12–20 m in the natural ground). Note that the
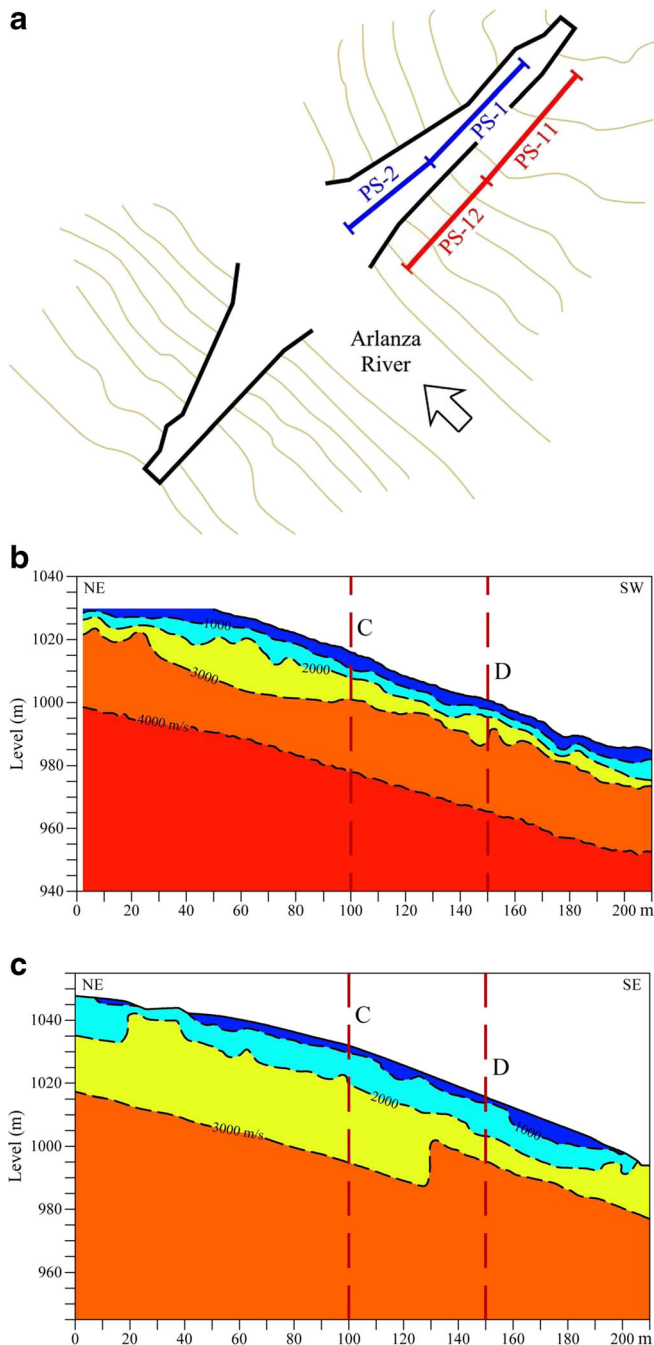
origin of the plot in Fig. 14 does not correspond to the same elevation for the two cases shown. If the plot for the excavated ground is displaced vertically downwards 10 m (the depth of the excavation), the straight lines describing the increase in seismic velocity in the undisturbed rock essentially coincide.

The profiles also show a very low value of (extrapolated) P-wave velocity at the surface. This is, in this case, an indication of the effect of lack of confining stress on wave velocity. In fact, V_p measures essentially the soil volumetric stiffness, which depends on the confining stress but also on the "quality" or degree of weathering of the material.

This double dependence makes it difficult to separate the two effects in a clear way. In this particular case, the Weald claystone foundation of the Castrovido dam in Burgos, core samples were recovered in several borings drilled from the abutment excavation and vertical profiles of water content and natural density with depth could be plotted. They are given in Fig. 15. Void ratio could be also calculated (γ_s=27–27.5 kN/m³). At depth, void ratio is close to 0.1 and it increases steadily when the surface is approached. At depths of 0–2 m, calculated values of void ratio range between 0.4 and 0.5.

The profiles of water content and density of Fig. 15 are reasonably consistent with the V_p plots versus depth (for the excavated ground) shown in Fig. 14. A weathering depth of about 6 m may be identified in Fig. 15. This weathering is the result of 3 years of exposure to atmospheric action and also the result of the large stress reduction implied by the abutment excavation.

Castrovido Weald claystone in its undisturbed state is a dense mixture of Calcite, Quartz, Muscovite, and Kaolinite. It has a low plasticity (w_L=24–35 %; PI=10–15 %) and its unconfined compression strength is rather variable (2–40 MPa). Strength and stiffness is lost at a fast rate when water content increases and this is shown in Fig. 16. The implication in terms of slope stability is the development of shallow failures. Instabilities are typically triggered by intense rainfall events but, in this case, the main factor was the slope deforestation which reduced the suction induced by the tree roots.

The preceding discussion indicates that two main effects control weathering: the atmospheric cycles (evaporation- and rainfall-induced wetting) and the confinement stress. An investigation of the damage induced by cycles of suction change at different isotropic confining pressures was reported by Pineda et al. (2013). Core samples of Lilla claystone, a similar low plasticity dense claystone to Castrovido, were subjected to stress-suction cycles paths involving different confining stresses and a varying intensity of suction change (Pineda et al. 2013). Sample stiffness was measured during testing by P- and S-wave transmission. Sample volumetric deformations were also monitored. Strength and pore size distributions were determined at the end of the cyclic suction changes.

A general damage rule could be established by relating the loss stiffness and strength with irreversible (plastic) volumetric expansion (Fig. 17). This rule may be used in constitutive models to simulate weathering effects. It shows that weathering effects may be related to a simple way to volumetric expansion, a result which was also present in the plots given in Fig. 16.

A final remark concerns the evolution of pore size distribution (Fig. 18b, e). The initial pore size distribution of the undisturbed specimens of Lilla claystone is essentially characterized by a monomodal distribution of very small pores. Suction cycles create
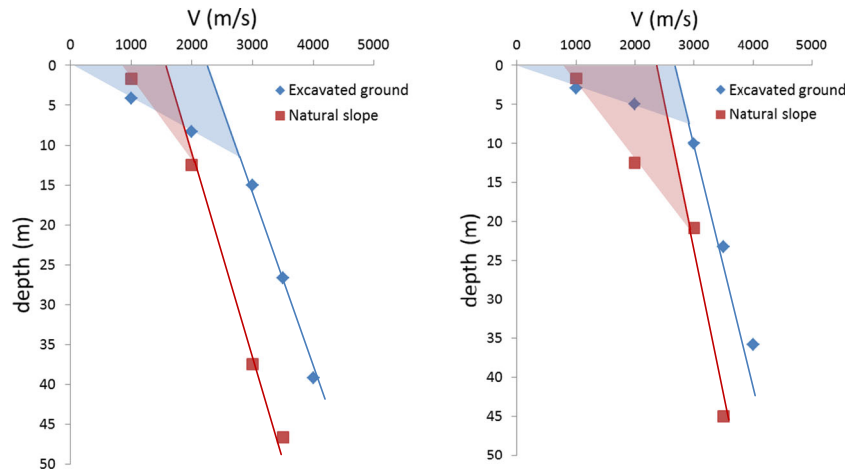

Fig. 13 a Arlanza Valley in Weald claystones and contours of Castrovido dam. Also indicated is the position of P-wave vertical profiles; P-waves seismic profiles: **b** PS-1 and PS-2 and **c** PS-11 and PS-12

Fig. 14 Vertical profiles of P-wave velocity in positions C and D (Fig. 16)

a family of very large pores (Fig. 18e). The practical implication is a significant increase in permeability. In fact, weathered soil profiles in a given claystone unit exhibit a decrease in permeability with depth. Often, definite weathering fronts are identified (Alonso et al. 2003). The associated sharp changes in permeability may explain the development of positive pore water pressures at the interfaces as a result of rainfall infiltration. These interfaces mark the position of shallow failure surfaces as discussed in detail in the previous reference.

Fig. 15 Castrovido Weald claystone. Variation with depth in the exposed excavation of **a** water content and **b** natural density. Symbols refer to different borings

Discontinuities

Two types of slope instability are present in the Castrovido dam area: shallow failures and planar failures controlled by sedimentation planes (Fig. 19). The photo shows the large excavation of the right abutment of the dam and a collapse of the downstream side of the excavation. The discontinuous lines show the dip of the sedimentation planes. At a large scale, the Weald formation is a sequence of claystone and interbedded sandstone layers although the claystone lithology dominates the sediments.

Slope stability and, indeed, the stability of the concrete gravity dam designed depend critically on the strength available in these sedimentation planes. Three types of contacts were identified in the course of a detailed field surveying campaign: sandstone–sandstone, sandstone–claystone, and planes inside the claystone. One significant aspect of this soft rock formation was the presence of Muscovite mica. Mica platelets were dispersed in the claystone matrix but they were often found also in some sedimentation planes inside the sandstone strata. The shear strength of stratification planes was investigated by direct shear tests at two scales: (a) tests were performed on block samples, up to 30×30 cm, recovered from several locations of the entire dam excavation area and (b) large-scale "in situ" tests, 80×80 cm in size.

Table 1 shows the results of the shear tests on block samples containing the plane being sheared. In all cases, the joints were saturated prior to shearing.

Residual conditions were approximated by applying a reversal loading cycle. The sandstone–sandstone contacts, when filled by mica sheets exhibited a ductile behavior and a low friction angle (ϕ=14°). However, they were not commonly found and sandstone–claystone contacts dominated the apparent behavior of the Weald formation at a large scale. These contacts were planar at the scale of the recovered blocks, and the data in Table 1 does not reflect the contribution of geometrical irregularities of the contacts beyond a certain scale.

This is better illustrated if one examines the roughness of a natural claystone–sandstone contact at a much larger scale (Fig. 20). The figure shows an uncovered contact during the preparatory works to locate the large-scale "in situ" shearing tests. Subvertical local fractures led a rough surface having abundant "jumps", difficult to characterize by a typical random roughness. The "in situ" shear tests were arranged to test the contact plane
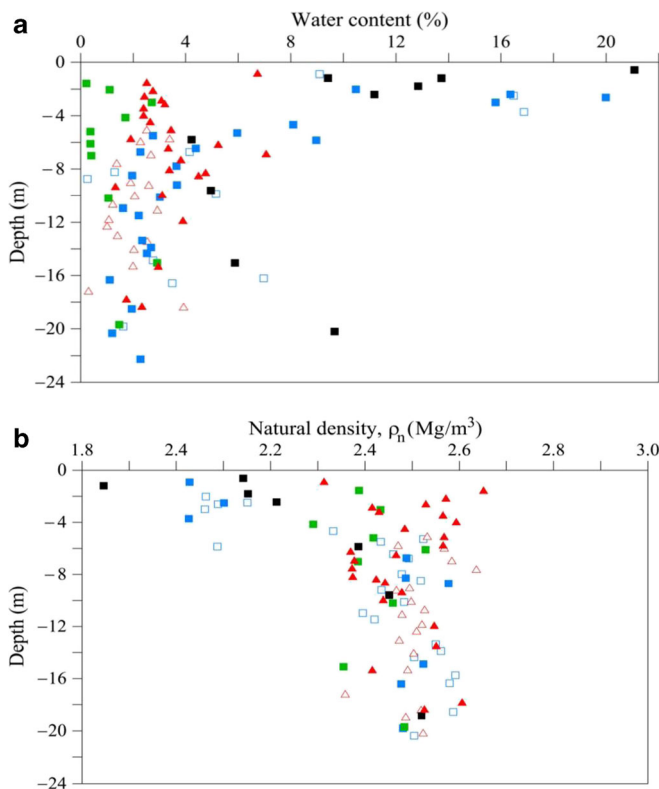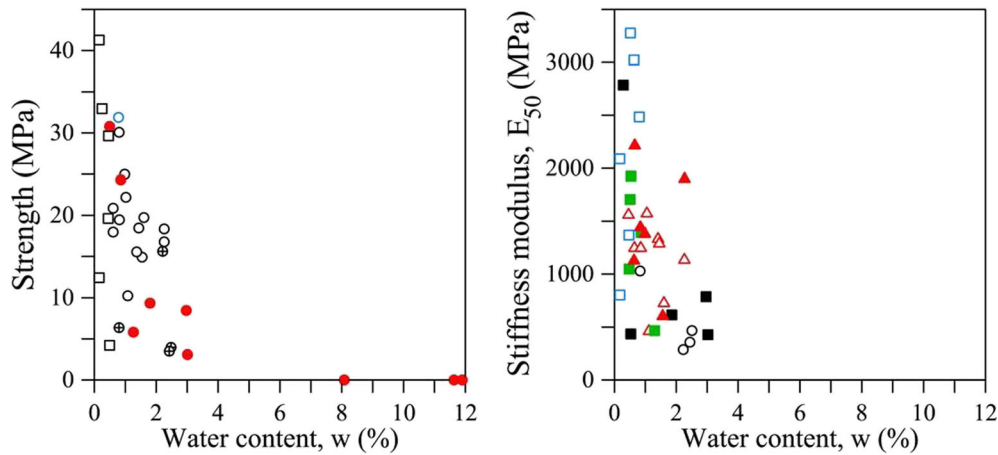
Fig. 16 Variation of unconfined strength and stiffness measured in cores recovered from the Weald formation in Castrovido. Symbols refer to different borings

shown in Fig. 20. Figure 20 also shows the tested plane in one of the six tests performed.

"In situ" tests were performed in a "staged" manner by applying an increasingly large normal stress and shearing the joint until limiting conditions for each normal stress applied. Shear displacements to reach the joint strength were very small (a few mm), as shown in Fig. 21, and the reduction of contact area was of no concern. The sheared plane was maintained under water during the test preparation and the shearing stage.

Tests were arranged in groups of three, close to each other, to minimize the effect of field variability. Despite this precaution, the strength envelopes exhibited significant differences. This is illustrated in Fig. 22, which summarizes the experiments performed at the 80×80 cm scale, as well as the tests on block samples (which provided in all cases linear envelopes and no apparent cohesion).

The most significant difference, when comparing the tests at the two different scales (80 cm "in situ" and 20–30 cm in the laboratory),

Fig. 17 Reduction of strength and stiffness with accumulated plastic deformation

was the nonlinear response of the "in situ" specimens that resulted in relatively high friction angles (but extremely variable) at low confining stresses (say lower than 0.2 MPa). An educated average strength envelope for the entire area is also shown in the figure.

The preceding results bring the question of scale effects when testing stratification surfaces. Figure 22, at normal stresses $\sigma_n <$ 0.2 MPa, indicates that the large "in situ" tests incorporate a more significant geometrical term in the measured strength. Hoek (2000) reported an empirical correction for scale effects on his joint roughness coefficient, JRC:

$$JRC_{Ln} = JRC_{Lo} \left(\frac{L_n}{L_o} \right)^{-0.02\,JRC_{Lo}} \tag{1}$$

Where JRC_{LO} is the roughness value for $L_o = 100$ mm and L_n is the "in situ" prototype length. This relationship is not supported by the preceding data. In fact, as an example, if $L_n = 10$ m and $JRC_{Lo} = 10°$, then $JRC_{Ln} = 4°$. This reduction in strength is not observed in the tests performed.

This case illustrates the significance of sedimentation surfaces in practice, especially when they explain or can be integrated into a critical failure mechanism. The large lateral extent and the possibility of pre-shearing have been widely recognized in the literature. The case discussed here highlights the difficulty to quantify the available strength even if a significant effort and economic resources are applied. An additional issue is the effect of scale, which is related to the particular geometrical details of the critical discontinuity surfaces.

The modification of strength after failure (landslide reactivation)

The residual friction angle is known to depend on rate effects but also on "state" effects. Ageing or healing has been reported to be a state effect leading to the progressive increase in residual friction angle during stability periods. Alonso (2012) provides a recent account of some experimental data on strength recovery in terms of "resting" time. Mesri and Huvaj-Sarihan (2012) question the gain in residual strength in resting periods. They believe that the gain observed in drained reversal shear box tests as well as in torsional shear tests is a consequence of spurious experimental results. However, the healing effect has often been observed when testing rock joints and gouge materials in faults (Karner et al. 1997; Marone 1997; Niemeijer and Spiers 2006). Mechanisms invoked to
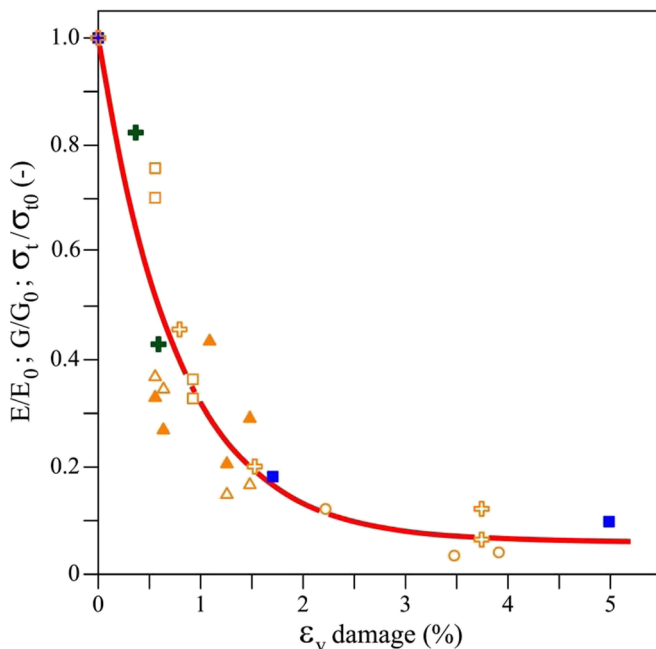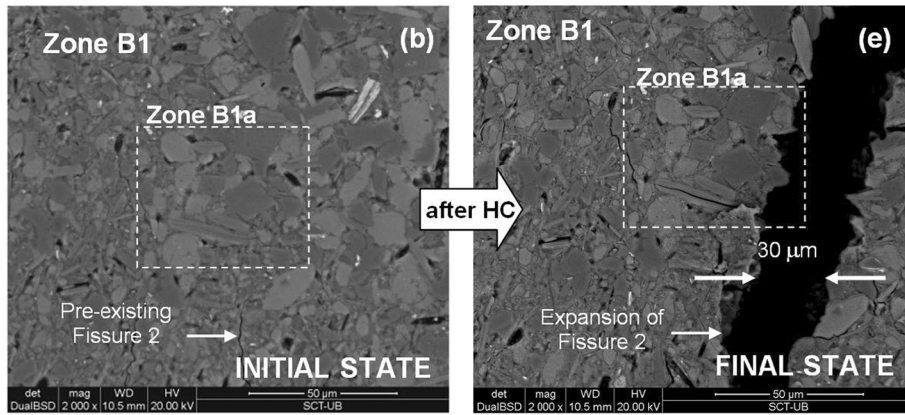
Fig. 18 SEM photomicrographs at **b** initial and **e** degraded states. After Pineda et al. (2013)

Fig. 19 Planar failure in Castrovido claystone controlled by sedimentation planes

explain the changes in friction during holding times are pressure solution of minerals, breakage, and deformation of particles (cataclasis) and foliation of phyllosilicates. The first and third mechanisms may be present in dormant slides in clayey soft rocks. This issue probably requires further examination.

An additional state effect is associated with chemical interactions on the failure surface. Strength may increase the accumulation of salt especially in coastal areas, precipitation of carbonates and iron compounds, and exchange of lower valence to higher valence cations

Table 1 Laboratory direct shear tests on block samples (up to 30×30 cm)

Type of interface	Peak friction angle	Residual friction angle
Sandstone–sandstone (mica contact)	14°	14°
Sandstone–claystone contacts	19°	13–18°
Planes inside the claystone	24°	14–20°

(Kenney 1967; Chandler 1969; Hutchinson 1969, 1970; Hawkins 1988; Moore 1991; Hawkins and McDonald 1992; Moore and Brunsden 1996; Anson and Hawkins 1998, 2002; Tiwari et al. 2005).

There are also mechanisms leading to the reduction of strength. They constitute a more serious challenge because they imply a long-term loss of safety. Alonso (1998), when reviewing a few reactivation landslides in low to medium plasticity clays, found that the back analyzed friction angle was systematically below values reported in well-known correlations (Lupini et al. 1981) between residual friction angle and a number of index tests. Figure 23, for instance, shows the position of four cases (Cortes, La Riba, Vallcebre upper and lower) on a plot relating residual friction and Plasticity Index. The four points lie below the correlations.

In one of the cases presented (Cortes), the thin shearing surface was located within a 2-m-thick marly layer of secondary origin. The "marl" was in fact a mixture of dolomite and quartz-crystals and kaolinite and illite clay particles. However, when the thin shearing band that constitutes the actual failure surface was analyzed by X-rays, dolomite was almost entirely absent. Shearing tests on the "marl" matrix and the shearing surface itself showed a

Fig. 20 Castrovido Weald form. Exposed sandstone–claystone sedimentation surface. Zoom-in of contact after in situ shearing test

difference of almost 5° in residual shearing friction (Alonso et al. 1993).

The process leading to the vanishing of dolomite crystals in the sliding surface is not clear. But a possibility advanced in Alonso et al. (1993) is the progressive dissolution of dolomite by acid rainwater after the first landsliding event. Hawkins et al. (1988) have shown that decalcification process lead to a reduction in residual friction. Whether the sliding surface is a preferential path for subsurface water or not is however not well documented. More recently, Thuro and Hatem (2010) tried to explain the historic Goldau fast landslide in Switzerland by a process of decalcification and loss of strength in the weathered marl where the rupture surface was located.

There are, however, other chemical processes that may also play a role. Shuzui (2001) analyzed the samples taken along the failure surface in Kunimi landslide. The failure surface was located in a hard mudstone. He found an increase in smectite content when moving from the top to the toe of the slide.

Azañón et al. (2010) reported the presence of bands of clay rich layers in the position of sliding surfaces of two landslides in shales and flysch in the south of Granada province, Spain. Smectite is the dominant mineral in these clay-rich layers. These authors, as well as Shuzui (2001), explain the mineralogical evolution of the clay-rich layers by establishing the balance relationship that regulates the concentration of different clay minerals. For instance, in the case of calcium montmorillonite and kaolinite:

$$6[Ca - \text{montmorillonite}] + 2CO_2 - 9H_2 \leftrightarrow 7[\text{kaolinite}] + Ca^{+2}$$
$$+ 2HCO_3^- + 8SiO_2 \qquad (2)$$
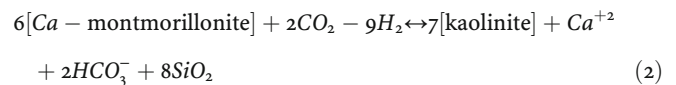
In the slides described by Azañón et al. (2010), carbonated rocks located at a higher elevation provide a continuous supply of calcified water which explains the abundance of Ca^{++} and CO_3H^- ions. Direct infiltration from rain also increases after
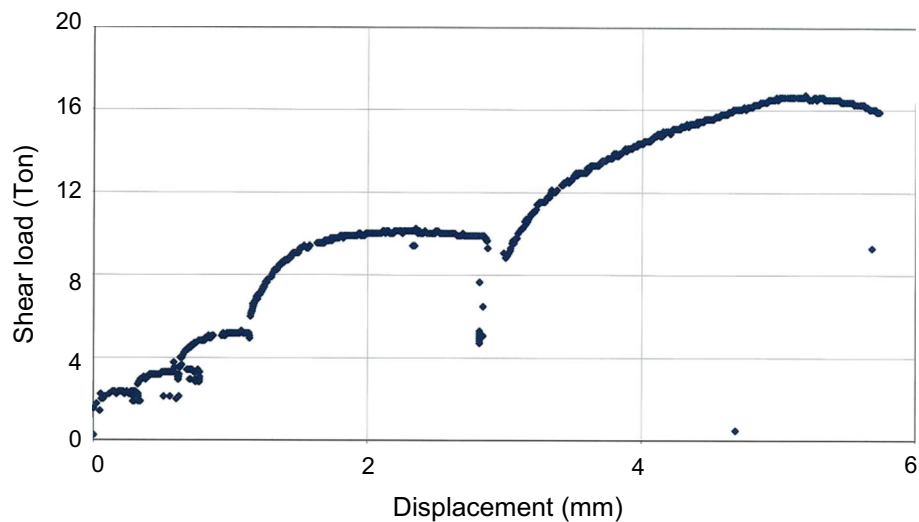

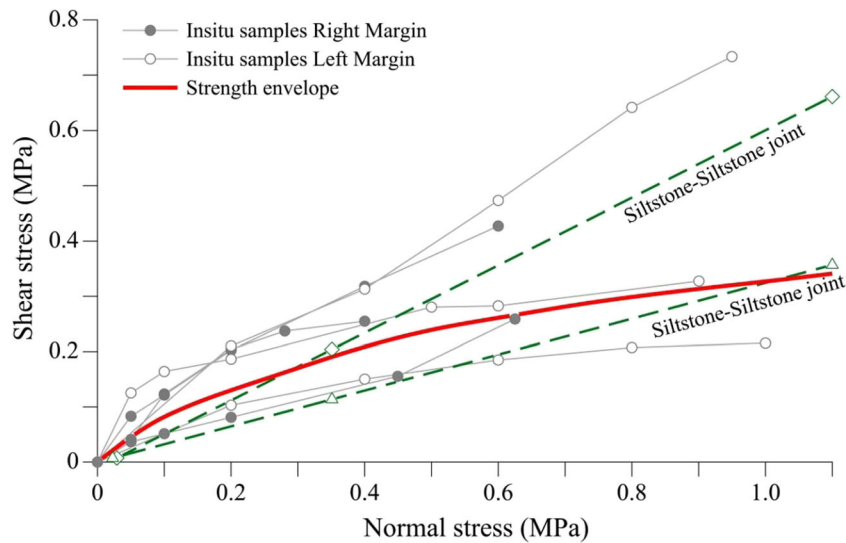**Fig. 21** Staged shearing of an "in situ" 80×80 cm sample

Fig. 22 Strength envelopes determined by different tests on claystone–sandstone sedimentation contacts. Castrovido Weald formation

instability because of the heterogeneous nature of the involved soils: a mixture of clay and blocks of different lithologies (marls, gypsum, limestone, and sandstones). In situ resistivity surveys indicated that the moving mass had a low resistivity if compared with nearby locations. This situation favors the water infiltration towards the sliding surface. Therefore, the hydrologically drive process contributes to leaching of carbonate minerals, increasing the Ca^{+2} and HCO_3^- ion concentration. This increase displaces the balance towards the left in the preceding equation and the montmorillonite concentration tends to increase. In practice, an increase in the contents of bicarbonate in the landslide water (when following the landslide slip surface) is correlated with an increasing content of montmorillonite.

The implication of these phenomena is clear for the analysis of the reactivation of landslides: it appears that the hydraulic regime established after an initial instability may lead to an increase in the clay content of the sliding surface and therefore to a reduction of the

Fig. 23 Bounds of residual friction angle reported by Lupini et al. (1981) and residual friction angles from back analysis of four actual failures described in Alonso (1998)

available residual friction. One of the practical problems associated with these phenomena is the difficulty to identify thin shearing bands by means of regular geotechnical surveying techniques.

Conclusions

Four main topics have been addressed:

– Brittleness and progressive failure in first time events

Progressive failure is probably a widespread phenomenon in first time failures although it is difficult to identify and measure in practice. There are no precise simple rules to select an engineering estimation of "average" strength explaining the initiation of failure. Examples given show that this average (limit equilibrium related) strength varies between the residual friction and an intermediate value between residual and peak friction angle. The precise determination of the failure process requires specific attention to a number of contributing aspects: initial stress state, process leading to the generation of the slope (excavation, loading, and stability problem), and its geometrical and time development, pore water pressure dissipation, constitutive soil model, and so on. Available computational tools have difficulties to handle these problems.

– Weathering

Weathering explains the occurrence of shallow slides. Physical weathering is controlled by confining stress and atmospheric cycles of suction (water content) changes. In stiff and dense claystones, weathering results in an increase in porosity and a very rapid decrease in stiffness and strength. In addition, permeability increases also in a significant way. As a result, the hydrologic response of the slide against rainfall action is controlled by the specific permeability profile. Weathering fronts are also a boundary separating zones of large permeability changes. Maximum pore water pressures localize at these boundaries, which then become a natural position for sliding surfaces.

– Discontinuities

Discontinuities are ever present in most of hard soils/soft rocks. Attention has been given to sedimentation planes in connection with a relatively involved field investigation to determine the available
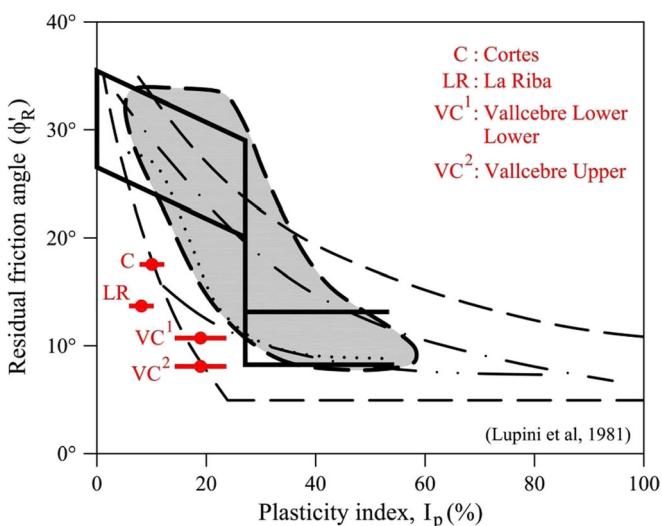
strength on the critical contacts between a softer material (a claystone) and harder layers (sandstone). The conclusion is rather pessimistic. Despite the effort, strength envelopes remain heterogeneous in an otherwise well-characterized geological unit. Large-scale "in situ" shear tests seem to be a good option, but, again, their reasonable size (in the order of 1×1 m) is not able to cope with the size of irregularities. The size or scale effect remains an open question.

–   Modification of strength after failure (landslide reactivation)

Field studies, progressively being published, indicate that the residual friction angle actually operating at the failure surface have experienced a significant change if compared with some original (or first time value). The examples mentioned indicate an increase in clay content in all cases and, therefore, a reduction in residual friction. The operating mechanism seems to be related to the dissolution of carbonates and to the parallel increase in clay minerals (in some cases montmorillonite, but not always).

The implication for practice is related to the difficulty of identifying in the field the thin shearing layer in which these phenomena have been active in the past.

References

Alonso E (1998) Cuttings and natural slopes. General report. The geotechnics of hard soils-soft rocks. A.A. Balkema 2:991–1000

Alonso EE (2012) 1st Heim Lecture: Deformation analysis of landslides: Progressive failure, rate effects and thermal interactions. Landslides and Engineered Slopes: Protecting Society through Improved Understanding. Taylor & Francis Group: 175–214

Alonso EE, Gens A (2006a) Aznalcóllar dam failure. Part 3: dynamics of the motion. Geotechnique 56(3):203–210

Alonso EE, Gens A (2006b) Aznalcóllar dam failure. Part I: field observations and material properties. Geotechnique 56(3):165–183

Alonso EE, Gens A, Lloret A (1993) The landslide of Cortes de Pallas, Spain. Geotechnique 43(4):507–521

Alonso E, Gens A, Delahaye CH (2003) Influence of rainfall on the deformation and stability of a slope in overconsolidated clays: a case study. Hydrogeol J 11:174–192

Anson RWW, Hawkins AB (1998) The effect of calcium ions in pore water on the residual shear strength of kaolinite and sodium montmorillonite. Geotechnique 48(6):787–800

Anson RWW, Hawkins AB (2002) Movement of the Soper's wood landslide on the Jurassic Fuller's Earth, Bath, England. Bull Eng Geol Environ 61(4):325–345

Azañón JM, Azor A, Yesares J, Tsige M, Mateos RM, Nieto F, Delgado J, López-Chicano M, Martín W, Rodríguez-Fernández J (2010) Regional-scale high-plasticity clay-bearing formation as controlling factor on landslides in SE Spain. Geomorphology 120:26–37

Bjerrum L (1967) Progressive failure in slopes of overconsolidated plastic clay and clay-shales. J Soil Mech Fdn Div Am Soc Civ Eng 93(SM5):3–49

Chandler RJ (1969) The effect of weathering on the shear strength properties of Keuper Marl. Geotechnique 19(3):321–334

Chandler RJ (1972) Lias clay: Weathering processes and their effect on shear strength. Geotechnique 22(3):403–431

Chandler RJ (1984) Delayed failure and observed strengths of first-time slides in stiff clays: a review. Proc. Intern. Symp. Landslides, Toronto, 2:19–25

Dixon N & Bromhead EN (1991) The mechanism of first-time slides in the London Clay cliff at the Isle of Sheppey, England. Int. Conf. Slope stability engineering: developments and applications, Isle of Wight, pp. 277–282

Gens A, Alonso EE (2006) Aznalcóllar dam failure. Part 2: stability conditions and failure mechanism. Geotechnique 56(3):185–201

Gens A, Ledesma A, Alonso EE (1996) Estimation of parameters in geotechnical backanalysis—II. Application to a tunnel excavation problem. Comput Geotech 18(1):29–46

Graham J, Au VCS (1985) Effects of freeze-thaw and softening on a natural clay at low stresses. Can Geotech J 22(1):69–78

Hawkins AB (1988) "Stability of inland soil slopes: some geological considerations ." 5th Int. Conf. on Landslides, Balkema, Netherlands, 1, 181–186

Hawkins AB, McDonald C (1992) Decalcification and residual shear strength reduction in Fuller's earth clay. Geotechnique 42(3):453–464

Hawkins AB, Lawrence MS, Privett KD (1988) Implications of weathering on the engineering properties of the Fuller's earth formation. Geotechnique 38(4):517–532

Hoek E (2000) Practical rock engineering. Published online www.rockscience.com

Hutchinson JN (1969) A reconsideration of the coastal landslides at folkestone warren, Kent. Geotechnique 19(1):6–38

Hutchinson JN (1970) A coastal mudflow on the London clay cliffs at Beltinge, north Kent. Geotechnique 20(4):412–438

Hutchinson JN (1988) Morphological and geotechnical parameters of landslides in relation to geology and hydrology. In: C. Bonnard (ed) Landslides. Proceedings of the 5th International Symposium on Landslides, volume 1, 3–35

Karner SL, Marone C, Evans B (1997) Laboratory study of fault healing and lithification in simulated fault gouge under hydrothermal conditions. Tectonophysics 277:41–45

Kenney TC (1967) "The influence of mineral composition on the residual strength of natural soils ." Proc., Geotechnology Conf. on Shear Strength Properties of Natural Soils and Rocks, NGI, Oslo, Norway, 1, 123–129

Lupini JF, Skinner AE, Vaughan PR (1981) The drained residual strength of cohesive soils. Geotechnique 31(2):181–213

Marone C (1997) On the rate of frictional healing and the constitutive law for time- and slip-dependent friction. Int J Rock Mech Min Sci 34(187):3–4

Mesri G, Abdel-Ghaffar MEM (1993) Cohesion intercept in effective stress stability analysis. J Geotech Eng ASCE 119(8):1229–1249

Mesri G, Huvaj-Sarihan N (2012) Residual shear strength measured by laboratory tests and mobilized in landslides. J Geotech Geoenviron 138(5):585–593

Mesri G, Shahien M (2003) Residual shear strength mobilized in first-time slope failures. J Geotech Geoenviron 129(1):13–31

Moore R (1991) The chemical and mineralogical controls upon the residual strength of pure and natural clays. Geotechnique 41(1):35–47

Moore R, Brunsden D (1996) Physico-chemical effects on the behaviour of a coastal mudslide. Geotechnique 46(2):259–278

Morgenstern NR (1977) Slopes and excavations in heavily overconsolidated clays. Proceed 9th ICSMFE, Tokyo 2:567–581

Niemeijer AR, Spiers CJ (2006) Velocity dependence of strength and healing behaviour in simulated phyllosilicate-bearing fault gouge. Tectonophysics 427:231–253

Pineda JA, Alonso EE, Romero E (2013) Environmental degradation of claystones. Geotechnique 64(1):64–82

Potts DM, Kovacevic N, Vaughan PR (1997) Delayed collapse of cut slopes in stiff clay. Geotechnique 47(5):953–982

Shuzui H (2001) Process of slip surface development and formation of slip surface clay in landslide in Tertiary volcanic rocks, Japan. Eng Geol 61:199–219

Skempton AW (1970) First time slides in over-consolidated clays. Geotechnique 20:320–324

Skempton AW, Petley DJ (1967) The strength along structural discontinuities in stiff clay. Proc Geot Conf Shear Strength Nat Soils and Rocks Oslo 2:3–20

Stark TD, Eid HT (1997) Slop stability analyses in stiff fissured clays. J Geotech Geoenviron Eng 123(4):335–343

Tavenas F, Leroueil S (1981) Creep and failure of slopes in clays. Can Geotech J 18(1):106–120

Terzaghi KV (1936) Stability of slopes of natural clay. Proc 1st Int Conf Soil Mech Found Eng 1:161–165

Thuro K and Hatem M (2010) The 1806 Goldau landslide event—analysis of a large rock slide. Geologically Active. Williams et al. (eds). Taylor & Francis: 3693–3700

Tiwari B, Tuladhar GR, Marui H (2005) Variation in residual shear strength of the soil with the salinity of pore fluid. J Geotech Geoenviron Eng 131(12):1445–1456

Wilson SD (1970) Observational data on ground movements related to slope instability. J of Soil Mechanics Found Eng, ASCE 96(SM5):1521–1544

Zabala F, Alonso EE (2011) Progressive failure of aznalcóllar dam using the material point method. Geotechnique 61(9):795–808

E. E. Alonso (✉) · N. M. Pinyol
Department of Geotechnical Engineering & Geosciences,
UPC-Campus Nord, c/ Jordi Girona 1-3, building D2, 2nd floor, office 206, Barcelona, 08034, Spain
e-mail: eduardo.alonso@upc.edu

N. M. Pinyol
International Center for Numerical Methods in Engineering, Campus Nord, C/ Gran Capitán s/n 08034, Barcelona, Spain